

Strong Visible Absorption and Broad Time Scale Excited-State Relaxation in $(\text{Ga}_{1-x}\text{Zn}_x)(\text{N}_{1-x}\text{O}_x)$ Nanocrystals

Chi-Hung Chuang,[†] Ying-Gang Lu,[†] Kyureon Lee,[†] Jim Ciston,[‡] and Gordana Dukovic^{*,†}

[†]Department of Chemistry and Biochemistry, University of Colorado Boulder, Boulder, Colorado 80309, United States

[‡]National Center for Electron Microscopy, Molecular Foundry, Lawrence Berkeley National Laboratory, Berkeley, California 94720, United States

S Supporting Information

ABSTRACT: $(\text{Ga}_{1-x}\text{Zn}_x)(\text{N}_{1-x}\text{O}_x)$ is a visible absorber of interest for solar fuel generation. We present a first report of soluble $(\text{Ga}_{1-x}\text{Zn}_x)(\text{N}_{1-x}\text{O}_x)$ nanocrystals (NCs) and their excited-state dynamics over the time window of 10^{-13} – 10^{-4} s. Using transient absorption spectroscopy, we find that excited-state decay in $(\text{Ga}_{0.27}\text{Zn}_{0.73})(\text{N}_{0.27}\text{O}_{0.73})$ NCs has both a short (<100 ps) and a long-lived component, with a long overall average lifetime of ~ 30 μs . We also find that the strength of the visible absorption is comparable to that of direct band gap semiconductors such as GaAs. We discuss how these results may relate to the origin of visible absorption in $(\text{Ga}_{1-x}\text{Zn}_x)(\text{N}_{1-x}\text{O}_x)$ and its use in solar fuel generation.

Converting and storing solar energy in chemical bonds is a desirable approach to renewable energy available on demand.¹ Solar fuels can be generated photoelectrochemically using semiconductors that harvest sunlight and allow photoexcited electrons to reduce H^+ or CO_2 and holes to oxidize water.² One of the major challenges in the quest for solar fuels is finding semiconductors that absorb visible light, have appropriate band edge energies for the reduction and oxidation half-reactions, and are resistant to photo-oxidation.^{2,3} Furthermore, a semiconductor that satisfies these requirements should have a sufficiently long excited state lifetime so that the photochemical pathways can compete with energy-wasting relaxation.

The oxynitride $(\text{Ga}_{1-x}\text{Zn}_x)(\text{N}_{1-x}\text{O}_x)$ has intriguing optical properties relevant to solar fuel generation. This solid solution of GaN and ZnO absorbs visible light, with the band gap determined by the value of x , even though both of the constituent semiconductors have band gaps >3 eV.⁴ When functionalized with a H^+ reduction co-catalyst, bulk $(\text{Ga}_{1-x}\text{Zn}_x)(\text{N}_{1-x}\text{O}_x)$ is capable of overall water-splitting under visible excitation.⁴ Moreover, this material is stable for months under water-splitting conditions.⁵ The origin of the composition-dependent visible absorption is not well understood. Proposed explanations include valence-band edge upshift due to mixing of ZnO and GaN orbitals, impurity level absorption, and interfacial absorption.^{6–13} This is a challenging question in part because electronic structure depends on compositional disorder (i.e., atomic-level connectivity of the four elements), which may depend on synthesis temperature and is difficult to measure experimentally.^{8,10,11}

We recently synthesized single-crystalline nanoparticles of $(\text{Ga}_{1-x}\text{Zn}_x)(\text{N}_{1-x}\text{O}_x)$ with a broad composition range ($0.3 < x < 0.87$) and absorption onsets that range from 2.7 eV for $x = 0.30$ to 2.2 eV for $x = 0.87$.¹⁴ A band gap of 2.2 eV corresponds to a maximum solar-to- H_2 conversion efficiency that approaches a highly desirable 15%, assuming a quantum efficiency of 100%.³ However, the highest reported apparent water-splitting quantum efficiency achieved with $(\text{Ga}_{1-x}\text{Zn}_x)(\text{N}_{1-x}\text{O}_x)$ is under 20%.¹⁵ The relaxation dynamics of the photoexcited carriers in this material are not well understood.¹⁵ Thus, it is not clear whether the low water-splitting quantum efficiency is a consequence of short carrier lifetimes inherent to this semiconductor or a reflection of materials properties, such as crystallinity and defects, that could be controlled via synthesis and processing.

Here, we report the measurement of excited-state dynamics in $(\text{Ga}_{1-x}\text{Zn}_x)(\text{N}_{1-x}\text{O}_x)$ nanocrystals (NCs) with $x = 0.73$ using transient absorption (TA) spectroscopy over a wide time window (10^{-13} – 10^{-4} s). $(\text{Ga}_{0.27}\text{Zn}_{0.73})(\text{N}_{0.27}\text{O}_{0.73})$ was chosen because ZnO-rich $(\text{Ga}_{1-x}\text{Zn}_x)(\text{N}_{1-x}\text{O}_x)$ compositions have smaller band gaps and are therefore more interesting for solar fuel generation.^{14–16} To enable the TA studies, we first solubilized $(\text{Ga}_{0.27}\text{Zn}_{0.73})(\text{N}_{0.27}\text{O}_{0.73})$ NCs in toluene using a long-chain organosilane. We directly measured the molar absorptivity in the visible and found it to be in the range of direct band gap absorption in semiconductors such as GaAs. TA spectra of solubilized $(\text{Ga}_{0.27}\text{Zn}_{0.73})(\text{N}_{0.27}\text{O}_{0.73})$ NCs had two main features: a UV bleach centered at 365 nm and a broad visible bleach centered at 425 nm. Both features had similar decay kinetics at early times (100 fs–3 ns), suggesting that they have similar electronic character. The decay of the visible bleach had both a fast (<50 ps) component and a long-lived component, with a very long average lifetime of ~ 30 μs . Along with the strong visible absorption, TA data are consistent with the theoretical predictions that visible absorption in ZnO-rich $(\text{Ga}_{1-x}\text{Zn}_x)(\text{N}_{1-x}\text{O}_x)$ originates from a transition between a valence band that arises from intermixing of ZnO and GaN and a conduction band that contains mostly Zn and O orbitals.^{6–8} We conclude with a discussion of how the optical properties reported here relate to potential applications of $(\text{Ga}_{1-x}\text{Zn}_x)(\text{N}_{1-x}\text{O}_x)$ in solar fuel generation.

The synthesis method that we developed for $(\text{Ga}_{1-x}\text{Zn}_x)(\text{N}_{1-x}\text{O}_x)$ NCs produces a powder of insoluble particles with no surface-capping ligands.¹⁴ Absorption spectra of such particles

Received: March 3, 2015

Published: May 2, 2015



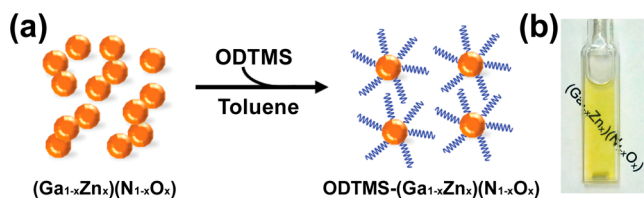


Figure 1. (a) Schematic representation of solubilization of $(\text{Ga}_{1-x}\text{Zn}_x)(\text{N}_{1-x}\text{O}_x)$ NCs using ODTMS. (b) Photograph of ODTMS-solubilized $(\text{Ga}_{0.27}\text{Zn}_{0.73})(\text{N}_{0.27}\text{O}_{0.73})$ NCs in toluene, illustrating that the solution is transparent and suitable for TA spectroscopy.

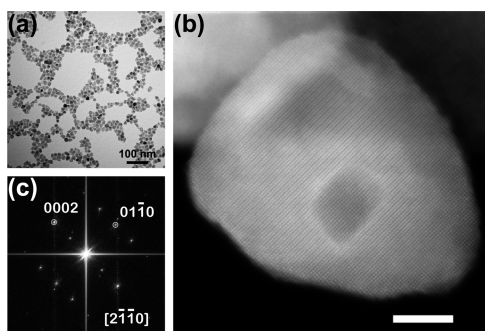


Figure 2. Characterization of solubilized $(\text{Ga}_{0.27}\text{Zn}_{0.73})(\text{N}_{0.27}\text{O}_{0.73})$ NCs by TEM. (a) Low-magnification bright-field TEM image showing particles with diameters of 15 ± 4 nm. (b) High-resolution STEM image of a selected NC, imaged along the $[2\bar{1}10]$ zone axis orientation. The scale bar is 5 nm. (c) Fourier transform pattern of the particle in (b), showing that the particle is a single wurtzite crystal.

can be determined by diffuse reflectance spectroscopy, but these samples are not transmissive and thus do not lend themselves easily to TA spectroscopy. To overcome this challenge, we first solubilized the particles in toluene using surface functionalization with octadecyltrimethoxysilane (ODTMS)¹⁷ (Figure 1a). The experimental details are described in section I of the Supporting Information (SI). We also used this method to solubilize ZnO NCs for the purposes of spectral comparisons. The solution of $(\text{Ga}_{1-x}\text{Zn}_x)(\text{N}_{1-x}\text{O}_x)$ NCs remains transparent for weeks to months (Figure 1b). Powder X-ray diffraction (XRD) shows a wurtzite crystal structure before and after solubilization with no significant change in particle size (~ 15 nm) (Figure S1).

Characterization of solubilized $(\text{Ga}_{0.27}\text{Zn}_{0.73})(\text{N}_{0.27}\text{O}_{0.73})$ NCs by transmission electron microscopy (TEM) is shown in Figure 2. The low-magnification TEM image (Figure 2a) shows well-dispersed particles with diameters of 15 ± 4 nm (Figure S3). The annular dark-field scanning TEM (STEM) image of a single $(\text{Ga}_{0.27}\text{Zn}_{0.73})(\text{N}_{0.27}\text{O}_{0.73})$ particle imaged along the $[2\bar{1}10]$ zone axis (Figure 2b) and its Fourier transform (Figure 2c) confirm the single-crystalline wurtzite structure. Thus, the solubilized particles resemble the as-prepared NCs both in crystallinity and in size.¹⁴ We note that the sizes of both $(\text{Ga}_{0.27}\text{Zn}_{0.73})(\text{N}_{0.27}\text{O}_{0.73})$ and ZnO particles (~ 10 nm) are too large for quantum confinement effects, as Bohr radii in both ZnO and GaN are < 3 nm.¹⁸

Spectral shape analyses have suggested that $(\text{Ga}_{1-x}\text{Zn}_x)(\text{N}_{1-x}\text{O}_x)$ is a direct band gap semiconductor,^{13,19} but the strength of the visible absorption has not been quantified. Access to solubilized particles allowed us to directly measure molar absorptivities (ϵ) of $(\text{Ga}_{0.27}\text{Zn}_{0.73})(\text{N}_{0.27}\text{O}_{0.73})$ and ZnO NCs by combining UV-vis absorption spectroscopy and elemental analysis. We report ϵ on a per metal cation basis (units of $\text{cm}^{-1} M_{\text{cation}}^{-1}$) to remove particle size as a variable (Figure 3).

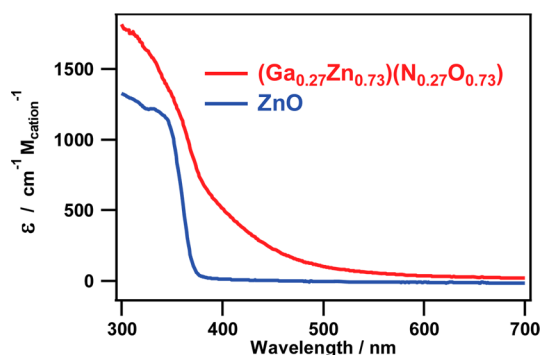


Figure 3. Molar absorptivities as a function of wavelength for solubilized $(\text{Ga}_{0.27}\text{Zn}_{0.73})(\text{N}_{0.27}\text{O}_{0.73})$ and ZnO NCs. The strength of the visible absorption is comparable to that of GaAs near the band gap.

ZnO and $(\text{Ga}_{0.27}\text{Zn}_{0.73})(\text{N}_{0.27}\text{O}_{0.73})$ NCs have comparable ϵ values of $\sim 1100 \text{ cm}^{-1} M_{\text{cation}}^{-1}$ at ~ 360 nm. $(\text{Ga}_{0.27}\text{Zn}_{0.73})(\text{N}_{0.27}\text{O}_{0.73})$ absorption in the visible is in the range of 100s of $\text{cm}^{-1} M_{\text{cation}}^{-1}$ and at ~ 450 nm is only a factor of 4 weaker than UV absorption. As another point of comparison, nanorods of CdS, a direct band gap semiconductor, have $\epsilon = 700 \text{ cm}^{-1} M_{\text{cation}}^{-1}$ at the quantum-confined band gap peak at 470 nm.²⁰ To compare the visible absorption strength in soluble $(\text{Ga}_{0.27}\text{Zn}_{0.73})(\text{N}_{0.27}\text{O}_{0.73})$ NCs to that of bulk semiconductors, we convert ϵ to the absorption coefficient α for a solid crystal (see section IV of SI). At 450 nm, $\epsilon = 227 \text{ cm}^{-1} M_{\text{cation}}^{-1}$ corresponds to $\alpha = 36\,000 \text{ cm}^{-1}$. This is comparable to GaAs, the direct band gap gold standard for photovoltaic devices, which has a value of α near the band gap on the order of 10^4 cm^{-1} .²¹ Thus, the strength of visible absorption of $(\text{Ga}_{0.27}\text{Zn}_{0.73})(\text{N}_{0.27}\text{O}_{0.73})$ is consistent with a direct band gap absorption rather than indirect or impurity-based transitions. In fact, the value of α measured here is similar to the theoretically predicted values for the direct band gap visible absorption in $(\text{Ga}_{1-x}\text{Zn}_x)(\text{N}_{1-x}\text{O}_x)$.^{6,22}

To describe the dynamics of photoexcited states in solubilized $(\text{Ga}_{0.27}\text{Zn}_{0.73})(\text{N}_{0.27}\text{O}_{0.73})$ NCs, we now turn to TA spectroscopy. As shown in Figure S4, the NC solution was stable, with no change in the absorption spectrum, for the duration of the TA experiments. Figure 4a shows TA spectra of $(\text{Ga}_{0.27}\text{Zn}_{0.73})(\text{N}_{0.27}\text{O}_{0.73})$ NCs at several delay times after pumping at 340 nm. We observe two strong features: an UV bleach peak centered at 365 nm and a broad bleach peak in the visible part of the spectrum, centered ~ 425 nm. For comparison, TA spectra of ZnO NCs pumped at 340 nm are shown in the inset of Figure 4a. ZnO exhibits the band gap exciton bleach centered at 365 nm and no features in the visible. The visible bleach in the $(\text{Ga}_{0.27}\text{Zn}_{0.73})(\text{N}_{0.27}\text{O}_{0.73})$ can also be induced with visible pump wavelengths. TA spectra with a 405 nm pump are shown in Figure 4b, and the visible bleach looks very similar to the one in Figure 4a.

To analyze the kinetics of excited-state relaxation, we first focus on the early times, 100 fs–3 ns. These kinetics were independent of pump power (Figure S5). Figure 5a shows the decay kinetics of $(\text{Ga}_{0.27}\text{Zn}_{0.73})(\text{N}_{0.27}\text{O}_{0.73})$ NCs at the peak of the UV and visible bleaches after pumping at 340 nm. Both the UV and the visible bleach show instrument-limited rise times (Figure S6), meaning that both bleach signals arise in < 500 fs. Remarkably, the UV and the visible bleaches decay in a very similar fashion. The kinetics of the visible bleach pumped at 405 nm are similar as well, as shown in Figure 5a. Each of these kinetics traces can be fitted with a biexponential decay with a fast

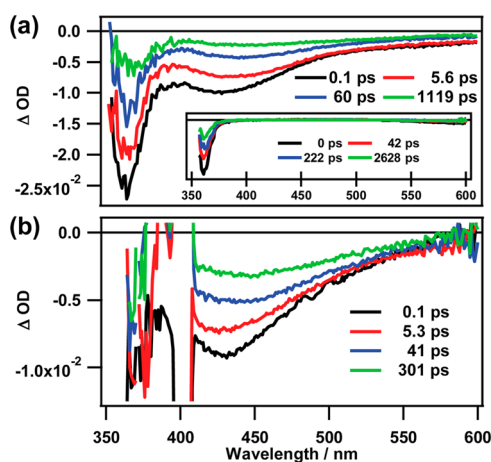


Figure 4. (a) TA spectra of $(\text{Ga}_{0.27}\text{Zn}_{0.73})(\text{N}_{0.27}\text{O}_{0.73})$ NCs at several delay times after pumping at 340 nm. Inset: equivalent TA spectra for ZnO NCs. (b) TA spectra of $(\text{Ga}_{0.27}\text{Zn}_{0.73})(\text{N}_{0.27}\text{O}_{0.73})$ NCs at several pump–probe delay times following pumping at 405 nm.

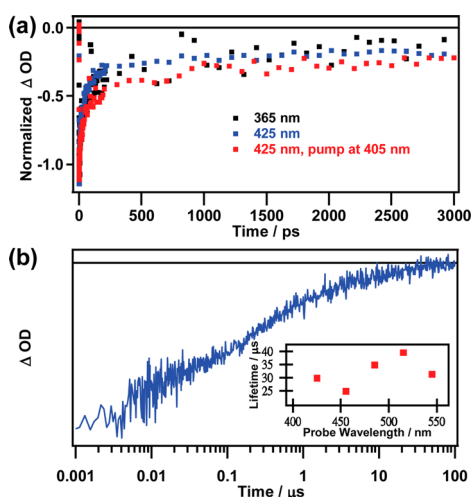


Figure 5. Excited-state relaxation in $(\text{Ga}_{0.27}\text{Zn}_{0.73})(\text{N}_{0.27}\text{O}_{0.73})$ NCs. (a) Normalized kinetics out to 3 ns probed at 365 and 425 nm following a 340 nm pump, and probed at 425 nm after a 405 nm pump. The decay traces for the UV and the visible bleaches are similar. (b) TA decay at 455 nm (pump = 340 nm) in the 1 ns–100 μs time window. Inset: average lifetimes as a function of wavelength.

decay component ranging from 15 to 30 ps, comprising $\sim 55\%$ of the total bleach amplitude (35% when pumped at 405 nm), and a longer component of several ns. The fitting parameters are shown in Table S2. The bleach decay kinetics of the $(\text{Ga}_{0.27}\text{Zn}_{0.73})(\text{N}_{0.27}\text{O}_{0.73})$ sample are qualitatively similar to the decay of the UV bleach of ZnO NCs (Figure S7), where the fast component is slightly longer, with a decay constant of 110 ps.

We next examine the fate of the visible bleach in the $(\text{Ga}_{0.27}\text{Zn}_{0.73})(\text{N}_{0.27}\text{O}_{0.73})$ sample that remains after the fast decay by considering the TA signal in the 1 ns–100 μs window (Figure 5b). Our white light probe in this time window does not extend into the UV, making the UV bleach not spectrally accessible. The decay kinetics of the visible bleach over this broad time window are nonexponential, as commonly observed with semiconductor NCs.²³ To calculate the average lifetime $\langle\tau\rangle$, we combined the short time scale and long time scale kinetics into one kinetic trace (Figure S8) and calculated $\langle\tau\rangle$ by integrating the TA signal using the definition:²⁴

$$\langle\tau\rangle = \frac{\int_0^{\infty} t\Delta A(t) dt}{\int_0^{\infty} \Delta A(t) dt} \quad (1)$$

The values of $\langle\tau\rangle$ vary from 25 to 40 μs over the visible range, as shown in the inset of Figure 5b. Because the definition of $\langle\tau\rangle$ weighs the long-lived decay components more heavily than short-lived ones, the fast 15–30 ps decay does not contribute strongly to $\langle\tau\rangle$. Compared with reported excited-state lifetimes in other materials of interest for solar fuel generation, such as BiVO_4 (~ 40 ns),²⁵ Fe_2O_3 (< 100 ps),²⁶ and Cu_2O (< 200 ps),²⁷ the average lifetime of $(\text{Ga}_{0.27}\text{Zn}_{0.73})(\text{N}_{0.27}\text{O}_{0.73})$ is longer by orders of magnitude.

We next address a possible assignment for the UV and visible bleach signals in $(\text{Ga}_{0.27}\text{Zn}_{0.73})(\text{N}_{0.27}\text{O}_{0.73})$ NCs (Figure 4). The similarities in the decay kinetics of the two bleaches (Figure 5a) suggest that the two signals share an electronic state. The instantaneous (within instrumental time resolution) population of both bleaches supports this assignment. A charge or energy transfer slower than 500 fs from the state corresponding to the UV bleach to the state corresponding to the visible bleach would manifest as a slower rise in the visible bleach. Because both bleaches correspond to strong absorption in the steady-state absorption spectrum (Figure 3), they most likely probe interband transitions, rather than impurity or defect states. Thus, the kinetics of the features in the TA spectra of $(\text{Ga}_{0.27}\text{Zn}_{0.73})(\text{N}_{0.27}\text{O}_{0.73})$ NCs suggest that the visible bleach shares the valence band or the conduction band with the UV bleach. It has been predicted theoretically that the conduction band in ZnO-rich $(\text{Ga}_{1-x}\text{Zn}_x)(\text{N}_{1-x}\text{O}_x)$ consists primarily of orbitals that originate from Zn and O, while the valence band arises from mixing in of Ga and N and lies higher in energy than the valence band of ZnO.^{6–8} Within that context, the absorption spectra in Figure 3 and bleach signals in Figure 4 would correspond to excitation of electrons into a conduction band that consists primarily of Zn and O orbitals, from a valence band that arises from the compositional mixing (transitions in the visible) as well as deeper lying levels (transitions in the UV). Based on the information currently available, this is a plausible assignment for the spectral signatures in $(\text{Ga}_{0.27}\text{Zn}_{0.73})(\text{N}_{0.27}\text{O}_{0.73})$ NCs, though we cannot completely rule out other possibilities at this time.

Further work is needed to reveal the relaxation mechanisms that correspond to the short 15–30 ps component comprising 55% of the excited-state decay in $(\text{Ga}_{0.27}\text{Zn}_{0.73})(\text{N}_{0.27}\text{O}_{0.73})$ NCs and the long-lived ($\langle\tau\rangle \approx 30$ μs) component making up the remaining 45% (Figure 5). These relaxation kinetics may play an important role in particle-based $(\text{Ga}_{1-x}\text{Zn}_x)(\text{N}_{1-x}\text{O}_x)$ architectures for solar water-splitting. In such systems, it is necessary to deliver the photoexcited electrons to the H^+ reduction co-catalyst, and the holes to the particle surface, where they oxidize water.⁴ Excited-state decay competes with these processes. If the productive pathways are slower than the fast decay process, the photochemical quantum efficiency is limited to the fraction of the excited states that decay by the slow process. It is possible that a fast excited-state decay component similar to the one observed here is responsible for the relatively low water-splitting quantum efficiencies observed with $(\text{Ga}_{1-x}\text{Zn}_x)(\text{N}_{1-x}\text{O}_x)$ materials.^{15,28}

The optical properties described here can also inform the design of photoelectrochemical (PEC) devices involving oxynitrides. Bulk $(\text{Ga}_{1-x}\text{Zn}_x)(\text{N}_{1-x}\text{O}_x)$ shows n-type behavior suitable for PEC water oxidation.²⁹ Let us suppose that single-crystalline $(\text{Ga}_{1-x}\text{Zn}_x)(\text{N}_{1-x}\text{O}_x)$ with variable thickness can be synthesized, and has absorption strength and excited-state

behavior similar to those of the $(\text{Ga}_{0.27}\text{Zn}_{0.73})(\text{N}_{0.27}\text{O}_{0.73})$ NCs described here. Based on the strength of the visible absorption, the absorption length ($1/\alpha$) of $(\text{Ga}_{0.27}\text{Zn}_{0.73})(\text{N}_{0.27}\text{O}_{0.73})$ at $\lambda = 450$ nm is 280 nm, so >95% of the incident light can be absorbed in a film that is <1 μm thick. Space-charge regions, in which separation of electrons and holes is fast and efficient, are normally on the order of 100s of nm wide.² This means that a PEC device that would absorb most of the incident light could consist mostly of the space charge region, in which mobile carriers can be separated as fast as picoseconds.³⁰ In this case, it is conceivable that even the short-lived excited-state components could be usable for PEC water oxidation. Provided that the photoexcited carriers probed here are reasonably mobile, PEC devices made of single-crystalline $(\text{Ga}_{1-x}\text{Zn}_x)(\text{N}_{1-x}\text{O}_x)$ with thickness of <1 μm may be of interest for solar fuel generation.

In conclusion, we present a first report of the excited-state decay in solubilized $(\text{Ga}_{0.27}\text{Zn}_{0.73})(\text{N}_{0.27}\text{O}_{0.73})$ nanocrystals, examining a broad time scale spanning 10^{-13} – 10^{-4} s. We found the strength of the visible absorption in $(\text{Ga}_{0.27}\text{Zn}_{0.73})(\text{N}_{0.27}\text{O}_{0.73})$ to be comparable to band gap absorption of direct semiconductors such as GaAs. This strong absorption is a positive attribute for PEC devices. Transient absorption spectra showed both a UV and a visible bleach. Both decayed with a fast (<100 ps) component and a long-lived component that resulted in an average lifetime of ~ 30 μs for the visible bleach. Our observations are consistent with theoretical predictions that visible absorption in $(\text{Ga}_{1-x}\text{Zn}_x)(\text{N}_{1-x}\text{O}_x)$ arises from band gap narrowing due to mixing of GaN and ZnO. The availability of soluble $(\text{Ga}_{1-x}\text{Zn}_x)(\text{N}_{1-x}\text{O}_x)$ NCs will enable further studies on the excited-state dynamics in this material, which we anticipate will provide insights into material design for solar fuel generation.

■ ASSOCIATED CONTENT

📄 Supporting Information

Sample preparation and characterization; XRD analysis; NC size measurements; estimation of α ; TA sample stability; pump-power dependence of TA kinetics; bleach rise kinetics; short timescale kinetic parameters; TA kinetics of ZnO NCs; full time scale TA kinetics. The Supporting Information is available free of charge on the ACS Publications website at DOI: 10.1021/jacs.5b02077.

■ AUTHOR INFORMATION

Corresponding Author

*gordana.dukovic@colorado.edu

Notes

The authors declare no competing financial interest.

■ ACKNOWLEDGMENTS

This work was supported primarily by a Beckman Young Investigators Award from the Arnold and Mabel Beckman Foundation, as well as by a Cottrell Scholar Award from Research Corporation for Science Advancement. ADF-STEM measurements were carried out at NCEM of Molecular Foundry at LBNL, supported by the Office of Science, Office of Basic Energy Sciences, of the U.S. Department of Energy under Contract No. DE-AC02-05CH11231. We thank C. Song and K. Bustillo for technical support at NCEM.

■ REFERENCES

(1) Lewis, N. S.; Nocera, D. G. *Proc. Natl. Acad. Sci. U.S.A.* **2006**, *103*, 15729.

(2) Walter, M. G.; Warren, E. L.; McKone, J. R.; Boettcher, S. W.; Mi, Q. X.; Santori, E. A.; Lewis, N. S. *Chem. Rev.* **2010**, *110*, 6446.

(3) Chen, Z. B.; Jaramillo, T. F.; Deutsch, T. G.; Kleiman-Shwarsctein, A.; Forman, A. J.; Gaillard, N.; Garland, R.; Takanabe, K.; Heske, C.; Sunkara, M.; McFarland, E. W.; Domen, K.; Miller, E. L.; Turner, J. A.; Dinh, H. N. *J. Mater. Res.* **2010**, *25*, 3.

(4) (a) Maeda, K.; Domen, K. *Chem. Mater.* **2010**, *22*, 612. (b) Maeda, K.; Teramura, K.; Lu, D. L.; Takata, T.; Saito, N.; Inoue, Y.; Domen, K. *Nature* **2006**, *440*, 295.

(5) Ohno, T.; Bai, L.; Hisatomi, T.; Maeda, K.; Domen, K. *J. Am. Chem. Soc.* **2012**, *134*, 8254.

(6) Huda, M. N.; Yan, Y. F.; Wei, S. H.; Al-Jassim, M. M. *Phys. Rev. B* **2008**, *78*, No. 195204.

(7) Jensen, L. L.; Muckerman, J. T.; Newton, M. D. *J. Phys. Chem. C* **2008**, *112*, 3439.

(8) Di Valentin, C. *J. Phys. Chem. C* **2010**, *114*, 7054.

(9) Yoshida, M.; Hirai, T.; Maeda, K.; Saito, N.; Kubota, J.; Kobayashi, H.; Inoue, Y.; Domen, K. *J. Phys. Chem. C* **2010**, *114*, 15510.

(10) Wang, S. Z.; Wang, L. W. *Phys. Rev. Lett.* **2010**, *104*, No. 065501.

(11) Li, L.; Muckerman, J. T.; Hybertsen, M. S.; Allen, P. B. *Phys. Rev. B* **2011**, *83*, No. 134202.

(12) McDermott, E. J.; Kurmaev, E. Z.; Boyko, T. D.; Finkelstein, L. D.; Green, R. J.; Maeda, K.; Domen, K.; Moewes, A. J. *Phys. Chem. C* **2012**, *116*, 7694.

(13) Lee, Y. C.; Lin, T. Y.; Wu, C. W.; Teng, H. S.; Hu, C. C.; Hu, S. Y.; Yang, M. D. *J. Appl. Phys.* **2011**, *109*, No. 073506.

(14) Lee, K.; Tienes, B. M.; Wilker, M. B.; Schnitzenbaumer, K. J.; Dukovic, G. *Nano Lett.* **2012**, *12*, 3268.

(15) Li, Y.; Zhu, L.; Yang, Y.; Song, H.; Lou, Z.; Guo, Y.; Ye, Z. *Small* **2015**, *11*, 871.

(16) Wang, J.; Huang, B.; Wang, Z.; Wang, P.; Cheng, H.; Zheng, Z.; Qin, X.; Zhang, X.; Dai, Y.; Whangbo, M.-H. *J. Mater. Chem.* **2011**, *21*, 4562.

(17) Pujari, S. P.; Scheres, L.; Marcelis, A. T. M.; Zuilhof, H. *Angew. Chem., Int. Ed.* **2014**, *53*, 6322.

(18) Senger, R. T.; Bajaj, K. K. *Phys. Rev. B* **2003**, *68*, No. 045313.

(19) Reinert, A. A.; Payne, C.; Wang, L.; Ciston, J.; Zhu, Y.; Khalifah, P. G. *Inorg. Chem.* **2013**, *52*, 8389.

(20) (a) Wilker, M. B.; Shinopoulos, K. E.; Brown, K. A.; Mulder, D. W.; King, P. W.; Dukovic, G. *J. Am. Chem. Soc.* **2014**, *136*, 4316. (b) Tseng, H. W.; Wilker, M. B.; Damrauer, N. H.; Dukovic, G. *J. Am. Chem. Soc.* **2013**, *135*, 3383.

(21) Nelson, J. *The Physics of Solar Cells*; Imperial College Press: London, 2003.

(22) Dou, M.; Persson, C. *Physica Status Solidi (a)* **2012**, *209*, 75.

(23) (a) Knowles, K. E.; McArthur, E. A.; Weiss, E. A. *ACS Nano* **2011**, *5*, 2026. (b) Jones, M.; Scholes, G. D. *J. Mater. Chem.* **2010**, *20*, 3533. (c) van Driel, A. F.; Nikolaev, I. S.; Vergeer, P.; Lodahl, P.; Vanmaekelbergh, D.; Vos, W. L. *Phys. Rev. B* **2007**, *75*, No. 035329.

(24) Lakowicz, J. R. *Principles of Fluorescence Spectroscopy*; Springer: New York, 2006.

(25) Abdi, F. F.; Savenije, T. J.; May, M. M.; Dam, B.; van de Krol, R. J. *Phys. Chem. Lett.* **2013**, *4*, 2752.

(26) Cherepy, N. J.; Liston, D. B.; Lovejoy, J. A.; Deng, H. M.; Zhang, J. Z. *J. Phys. Chem. B* **1998**, *102*, 770.

(27) Paracchino, A.; Brauer, J. C.; Moser, J. E.; Thimsen, E.; Graetzel, M. *J. Phys. Chem. C* **2012**, *116*, 7341.

(28) Maeda, K.; Teramura, K.; Domen, K. *J. Catal.* **2008**, *254*, 198.

(29) (a) Ahn, K.-S.; Yan, Y.; Shet, S.; Deutsch, T.; Turner, J.; Al-Jassim, M. *Appl. Phys. Lett.* **2007**, *91*, No. 231909. (b) Hashiguchi, H.; Maeda, K.; Abe, R.; Ishikawa, A.; Kubota, J.; Domen, K. *Bull. Chem. Soc. Jpn.* **2009**, *82*, 401.

(30) Tan, M. X.; Laibinis, P. E.; Nguyen, S. T.; Kesselman, J. M.; Stanton, C. E.; Lewis, N. S. *Progress in Inorganic Chemistry*; John Wiley & Sons, Inc.: New York, 2007; Vol. 41, p 21.